

VALIDATION OF GLOBAL SOLAR RADIATION MODELS ON A HORIZONTAL SURFACE IN THE CLIMATIC ZONES OF BURKINA

ABSTRACT

The evaluation of the solar deposit is essential for the sizing of photovoltaic systems. This requires the availability of radiation data. In Burkina Faso, weather data doesn't cover all the country. That makes that solar radiation measured are not available for the all country. Theoretical methods can help about it. This paper is written to fill the gap of adapted solar models for the country. In this work, an analysis of the results provided by four models for the estimation of hourly values of global radiation on a horizontal plane was made. The radiation data for the year 2017 comes from the Burkina weather forecast. The validation of the models is carried out by a comparison between the radiation measured and that given by the various models provided by MATLAB code. The different models have been validated by several statistical indicators (RMSE and normalized MAE) and graphs for a clear sky. Scoring criteria have been established to assess the relative quality of each model. The models retained for the study are the Bird and Hulstrom model, the Davy and Hay model, the Capderou model and the Liu and Jordan model. Three sites were affected: Ouagadougou, Dori and Gaoua. We found that for some models, there is a good agreement between the measured values and those estimated by some models for the Dori site, while they are not with the values measured for the Ouagadougou and Gaoua sites. In the town of Dori, the most appropriate model for estimating solar radiation is that of Bird and Hulstrom. For the cities of Ouagadougou and Gaoua, the different models are not suitable.

Keywords: solar radiation, semi-empirical model, statistical indicators; estimate

1. INTRODUCTION

Of all the forms of energy, solar energy is the most abundant inexhaustible energy resource on earth, it represents the main source of energy for the earth-atmosphere system [1]. The random and discontinuous aspect of solar energy as well as the phase shift of its availability, in time, compared to the needs of energy exploitation, shows the importance and the need to know the solar deposit [2]. Its use at a given site and the optimization of its collection are the starting point for any investigation in the field of solar and bioclimatic architecture. This requires knowledge of the distribution of solar irradiation which is a function of several geographical, meteorological and astrological parameters [3]. Knowing the solar potential requires measurements. Sunshine data is collected annually by meteorological stations around the world, but the distribution of its stations does not generally cover the entire territory of the country. In

the metrology of solar potential, many methods are used, instrumentation on the ground but also in space by satellite. Data collected contribute to elaborate theoretical models([4],Burkina Faso, with a sunshine potential estimated at an average of 5.5 kWh/m²/day for a sunshine duration varying between 3000 and 3500 h/year, can considerably reduce its fossil energy bill by turning to the production of solar energy [5]. Thus, data collected for a locality are most often extrapolated to an entire region where there may be microclimates. Standard values are therefore defined at the scale of a region or a country to size solar collectors and to size cooling or heating needs in the homes. This situation can lead to oversizing of solar equipment. Developing tools and technics to have more precise data becomes imperative if we want to achieve better sizing and thus move towards energy savings, in particular in solar and bioclimatic architecture. By not being able to install meteorological stations over the entire extent of a territory, the use of the theoretical model is interesting insofar as they make it possible to have local data and this with reduced costs. That is why, an overview of solar radiation modeling is important. The studies on the estimation of solar radiation already carried out in Burkina ([4],[5], [6], [7].), do not provide standard models for all regions. Many models make it possible to reconstruct the components of solar radiation ([8], [9],...). The objective of this study is to fill the gap of adapted solar models for the country by analyzing the response of four models in relation to the measurements made by the national meteorological service for the year 2017. This analysis leads to the use of different models depending on the geographical position of the cities studied (Model of Bird & Hulstrom, model of Davies & Hay, model of Capderou and that of Lui and Jordan). More specifically it will be:

- Study and compare global radiation on a horizontal plane with measurements made by the weather forecast,
- Choose the one that is most suitable for each city.

2. MATERIAL AND METHODS

2.1 Methodology

Among the models for estimating radiation, those which are semi-empirical, have a local character and make it possible to calculate the direct, diffuse and global components [10]. In Burkina Faso, the national meteorological agency has about ten measuring stations in the country. The country is subdivided into three (03) climatic zones. In our study, we used data measurements of global irradiation on an hourly scale for the sites of Ouagadougou, Gaoua and Dori. The choice of these sites was based on the availability of the radiometric data sought and on the difference in climate between them. The geographical characteristics of the sites studied are given in table 1 below and figure 1.



Figure 1 : Geographical Location of the Cities Studied

Table 1 : Geographical coordinates of the sites used

Cities	Gaoua	Ouagadougou	Dori
Latitude	10°17'57" North	12°21'56" North	14°02'07" North
Longitude	3°15'02" West	1°32'01" West	0°02'04" West
Altitude (m)	329	296	277
Climatic zone	Sudanian zone	Sudano-Sahelian zone	Sahelian zone

The data from the weather station file is 15-minute time step data. We opted to keep the hourly data for the simulation. For each month of the year, a day was chosen based on the typical monthly day (defined by a characteristic declination) and which has daily irradiation equal to the monthly average [7]. In our study, the determination of the days was done initially by observing the shape of the sunshine curves on the Excel software. Secondly, when the shape of the curve is good, we check the status of the day on the Giovanni site [Giovanni \(nasa.gov\)](https://giovanni.gsfc.nasa.gov/)[11]. Otherwise, the day is replaced by a day of the same month which has better characteristics on the site.

To obtain a validation of solar radiation, a comparison between the estimates of the four radiation models on the horizontal plane, delivered by the Matlab program calculation code in clear skies and the solar radiation provided by the Burkina meteorological station for the year 2017, was made over a period covering the whole year to have a high representativeness of the results. But significant results are given for one month of a quarter. The results of the simulations carried out were first compared graphically in the form of representative curves with the measured values and those estimated by each of the models.

2.2 Statistical indicators

To evaluate these simulations from a statistical point of view, we calculated the most used scores for evaluate estimation models. It is:

- The Mean Absolute Error (MAE) is a measure of errors between paired observations expressing the same phenomenon. It is calculated by the following relationship:

$$MAE = \frac{\sum_i^N |Val_{me} - Val_{es}|}{N} \quad (1)$$

Val_{me} : average of measured values

Val_{es} : mean of simulated values

N : Number of value

- The Mean Squared Error or Root Mean Square Error is the standard deviation of the residuals (prediction errors) and is given by the following formula:

$$RMSE = \sqrt{\frac{\sum (Val_{me} - Val_{es})^2}{N}} \quad (2)$$

With two dispersion measures such as RMSE and MAE and three normalization means, there are six possible methods to calculate the percentage error [12]. Of these six (06) possible methods to calculate the percentage of error, those using the average radiant energy were exploited.

- Normalized RMSE (NRMSE) is calculated as follows:

$$NRMSE = \frac{RMSE}{\overline{Val_{me}}} \quad (3)$$

$\overline{Val_{me}}$: average of measured values

- Normalized MAE (NMAE) is calculated as follows:

$$NMAE = \frac{MAE}{\overline{Val_{me}}} \quad (4)$$

Of these two normalized quantities, the NMAE provides the best practical measure of relative dispersion error based on the selected endpoints and subjective assessments [12].

2.3 Description of study models

Table 2: Description of the models selected for the estimation of diffuse and global direct solar radiation on a horizontal plane.

Authors	Model equations	Type
---------	-----------------	------

Bird & Hulstrom [13], [10]	$I_{BH} = 0,975 \times I_{SC} \times \tau_r \times \tau_g \times \tau_o \times \tau_w \times \tau_a \times \cos \theta_z$	Direct
	$D_{BH} = D_r + D_a + D_m$	Diffuse
	avec	
	$D_r = 0,79 I_0 \cos \theta_z \times \tau_0 \times \tau_g \times \tau_w \times \tau_{aa} \times 0,5 \times \frac{1 - \tau_r}{1 - m_a - m_a^{1,02}}$	
	$D_a = 0,79 I_0 \cos \theta_z \times \tau_0 \times \tau_g \times \tau_w \times \tau_{aa} \times F_c \times \frac{1 - \tau_{as}}{1 - m_a - m_a^{1,02}}$	
	$D_m = (I + D_r + D_a) \rho_g \frac{\rho_a}{1 - \rho_g \rho_a}$	
	$G_{BH} = I_{BH} + D_{BH}$	Global
Davies and Hay [14], [15], [16]	$I_{DH} = I_{SC} (\tau_0 \tau_r - \alpha_w) \tau_a \cdot \cos \theta_z$	Direct
	$D_{DH} = D_r + D_a + D_m$	Diffuse
	Avec	
	$D_r = I_{SC} \tau_0 \tau_a (1 - \tau_r) \times 0,5 \cos \theta_z$	
	$D_a = I_{SC} (\tau_0 \tau_r - \alpha_w) [F_c \omega_0 (1 - \tau_a)] \cos \theta_z$	
	$D_m = (I + D_a + D_r) \frac{\rho \rho_a}{1 - \rho \rho_a}$	
	$G_{DH} = I_{DH} + D_{DH} = (I + D_r + D_a) \times \frac{1}{1 - \rho \rho_a}$	Global
Capderou [10], [17], [18]	$I_{CD} = I_0 C_{t-s} \sinh \left[\frac{-T_L}{0,9 + \frac{9,4}{0,89^z} \times \sinh} \right]$	Direct
	$D_{CD} = C_{sj} \times \exp \left\{ -1 + 1,06 \times \log(\sinh) + a - \sqrt{a^2 + b^2} \right\}$	Diffuse
	Avec	
	$a = 1,1$ et $b = \log(T_L - T_w) - 2,8 + 1,02(1 - \sinh)^2$	Global
	$G_{CD} = I_{CD} + D_{CD}$	
Liu et Jordan [18]	$I_{LJ} = I_h = A \sin(h) \exp \left(\frac{-1}{C \sin(h+2)} \right)$	Direct
	$D_{LJ} = D_h = B (\sin(h))^{0,4}$	Diffuse
	$G_{LJ} = I_{LJ} + D_{LJ} = I_h + D_h$	Global

3. RESULTS AND DISCUSSION

By quarter, the graphical results of a single month are represented. But, three types of curves are represented for four (04) months of the year. These are the curves given by the different models and those of the weather, the curves of the relative errors for each model and the curves of the different models according to the measured data.

3.1 RESULTS

3.1.1 In the City of Dori

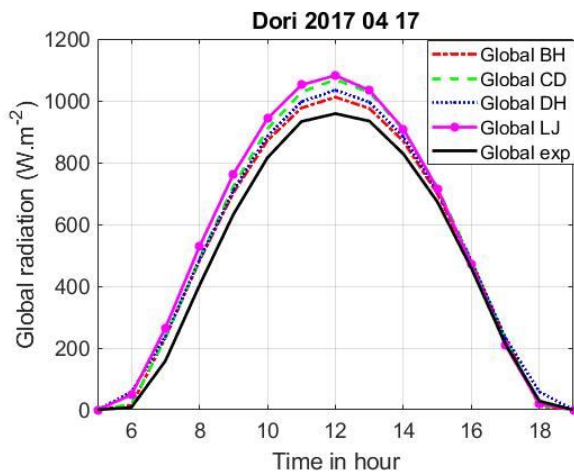


Figure 2: Comparison between the measured radiation and the simulated radiation of the three (03) theoretical models on 04/17/2017 in Dori

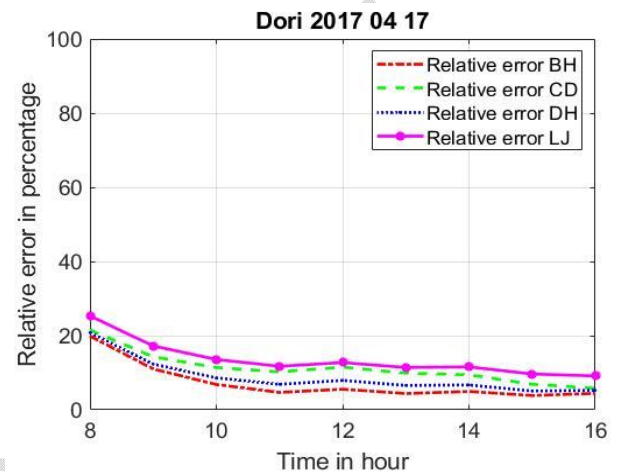


Figure 3: Relative error between the measured radiation and the simulated radiation of the three (03) models on 04/17/2017 in Dori

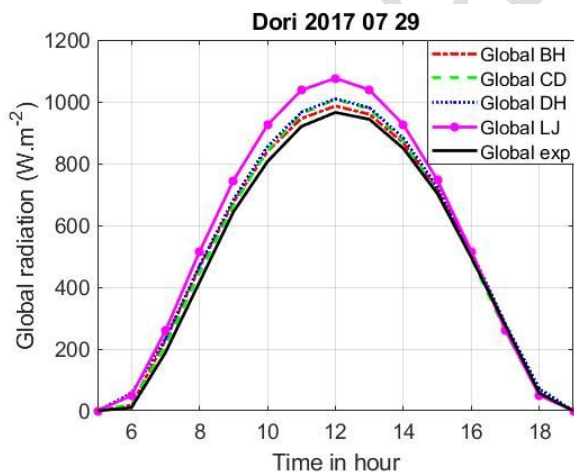


Figure 4: Comparison between the measured radiation and the simulated radiation of the three (03) theoretical models on 07/29/2017 in Dori

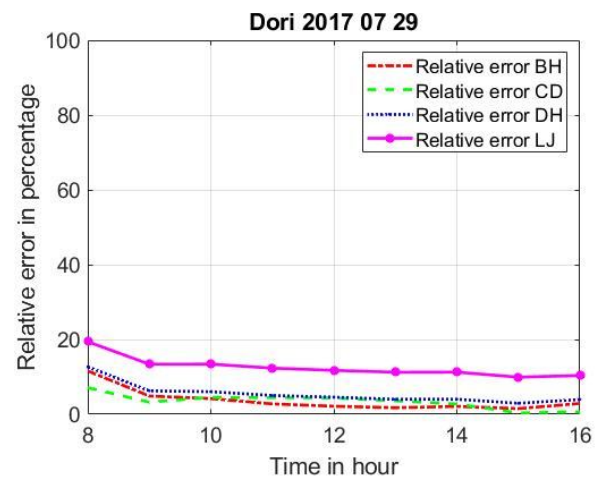


Figure 5: Relative error between the measured radiation and the simulated radiation of the three (03) models on 07/29/2017 in Dori

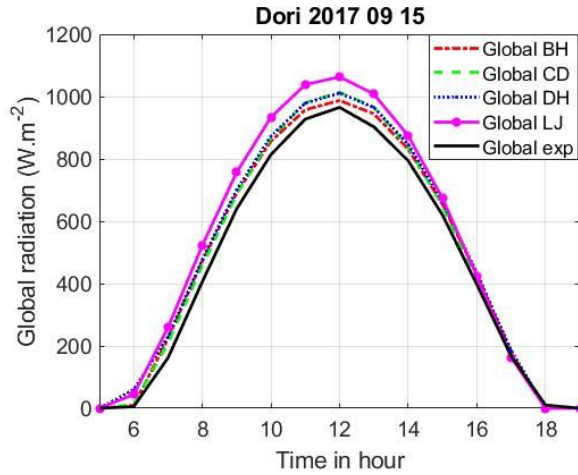


Figure 6: Comparison between the measured radiation and the simulated radiation of the three (03) theoretical models on 09/15/2017 in Dori

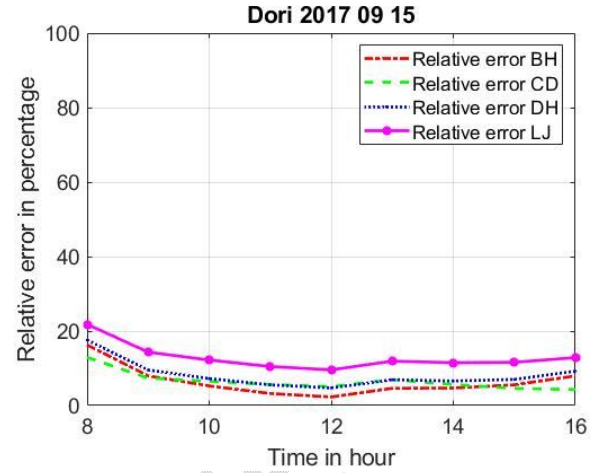


Figure 7: Relative error between the measured radiation and the simulated radiation of the three (03) models on 09/15/2017 in Dori

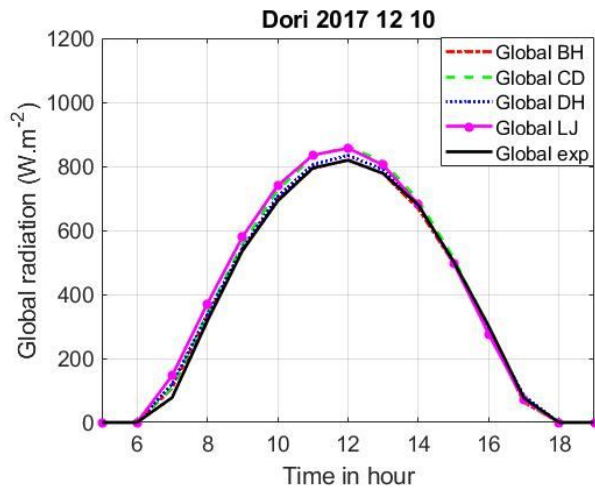


Figure 8: Comparison between the measured radiation and the simulated radiation of the three (03) theoretical models for the day of 18/01/2017 in Dori

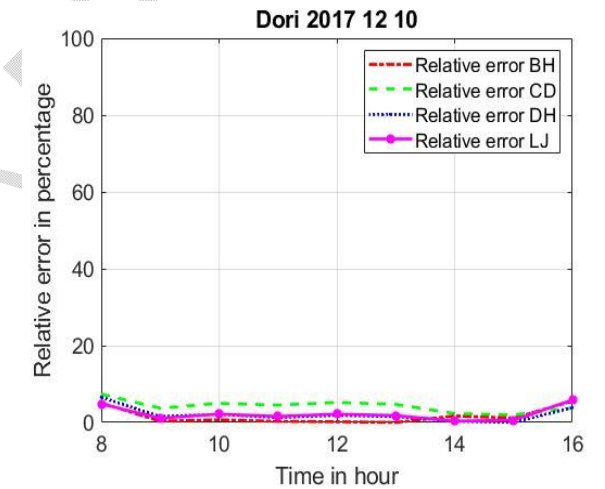


Figure 9: Relative error between the measured radiation and the simulated radiation of the three (03) models on 01/18/2017 in Dori

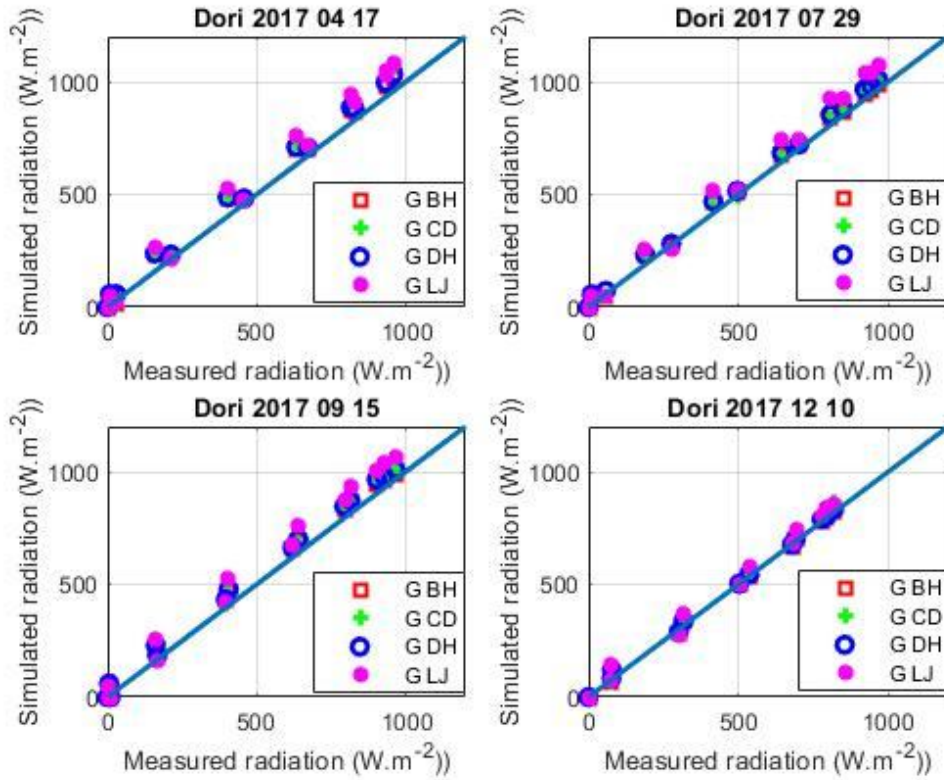


Figure 10: Simulated radiation versus measured radiation for the city of Dori

3.1.2 In the City of Ouagadougou

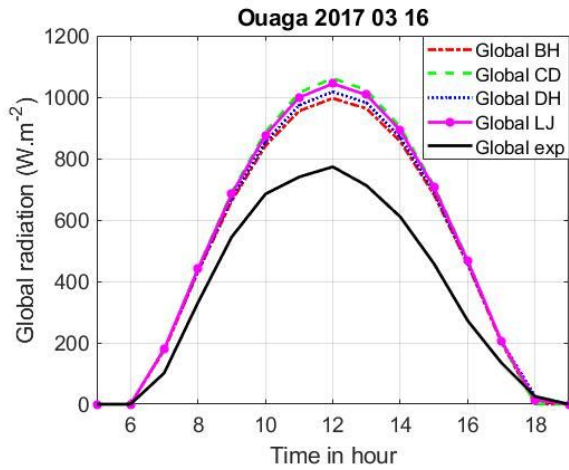


Figure 11: Comparison between the measured radiation and the simulated radiation of the three (03) theoretical models on 03/16/2017 in Ouaga

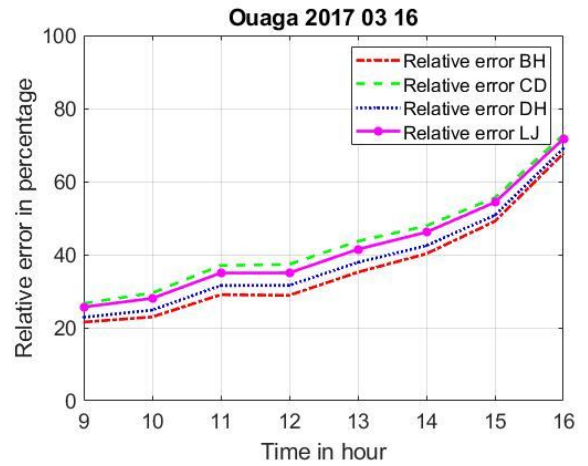


Figure 12: Relative error between the measured radiation and the simulated radiation of the three (03) models on 03/16/2017 in Ouaga

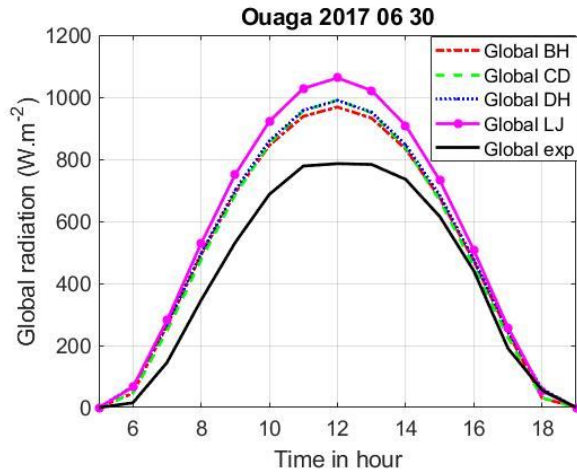


Figure 13: Comparison between the measured radiation and the simulated radiation of the three (03) theoretical models on 06/30/2017 in Ouaga

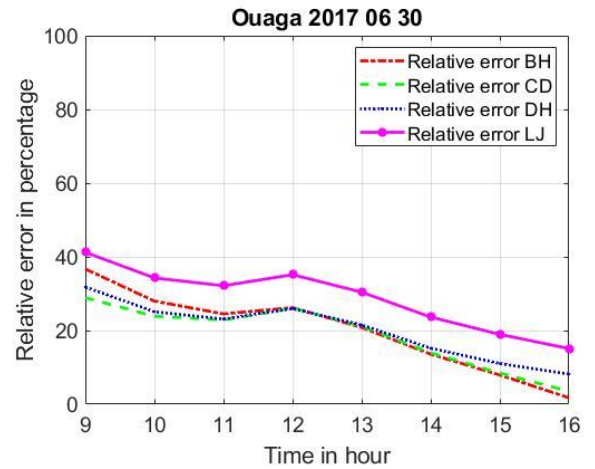


Figure 14: Relative error between the measured radiation and the simulated radiation of the three (03) models on 06/30/2017 in Ouaga

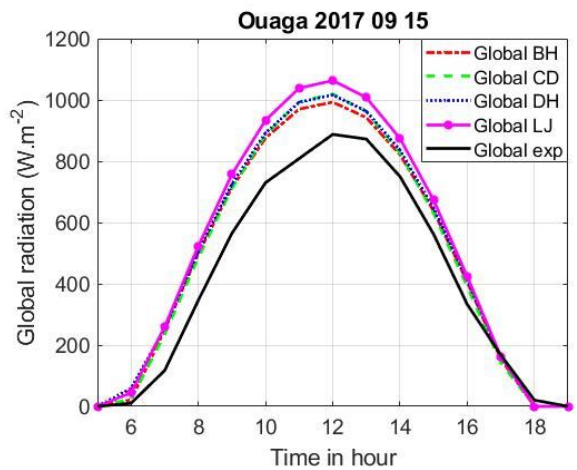


Figure 15: Comparison between the measured radiation and the simulated radiation of the three (03) theoretical models on 09/15/2017 in Ouaga

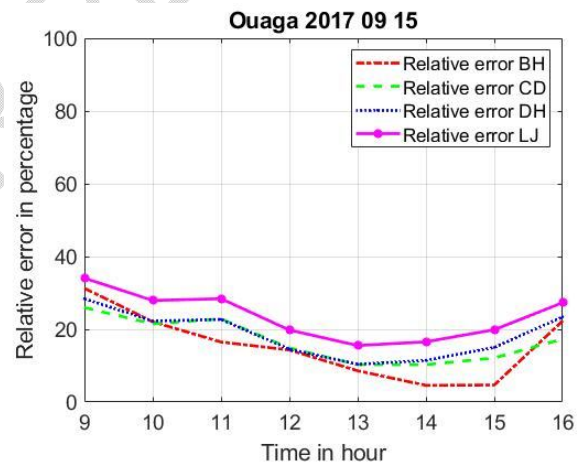


Figure 16: Relative error between the measured radiation and the simulated radiation of the three (03) models on 09/15/2017 in Ouaga

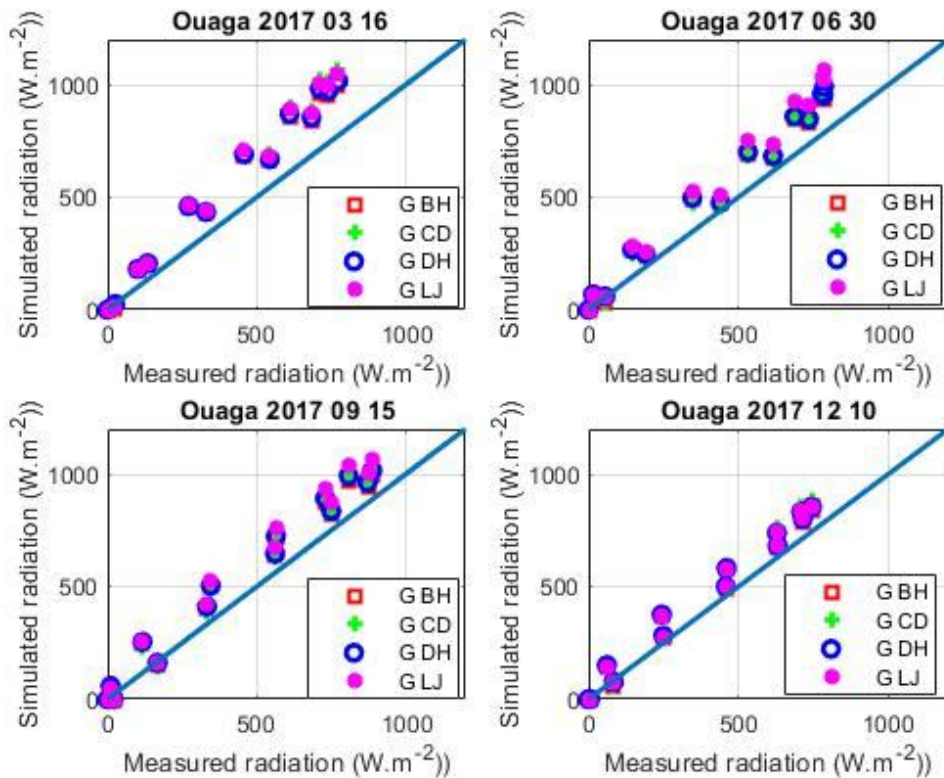
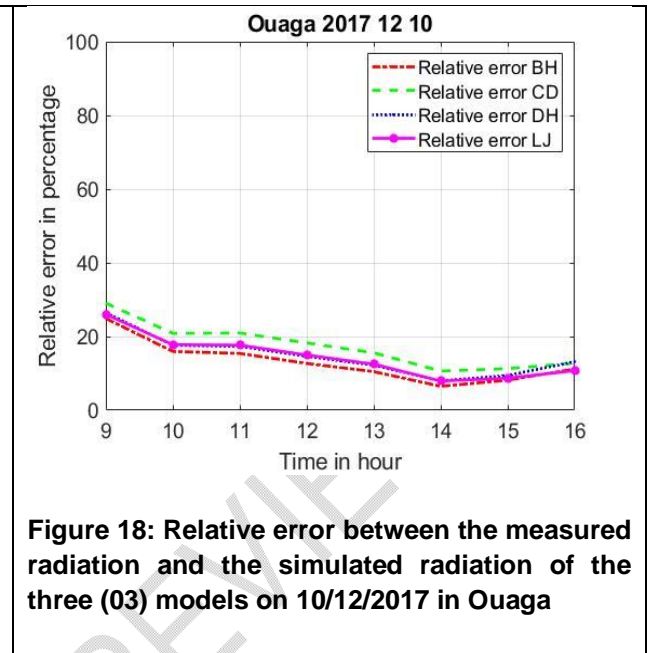
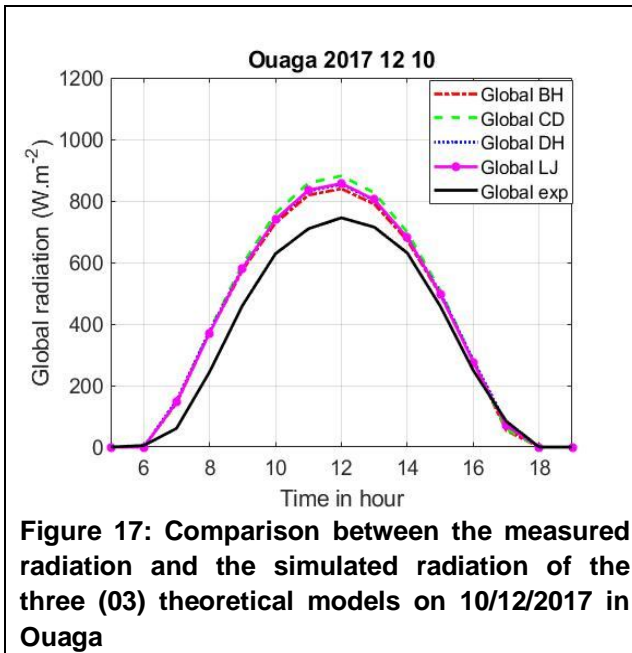


Figure 19: Simulated radiation as a function of measured radiation for the city of Ouaga

3.1.3 In the City of Gaoua

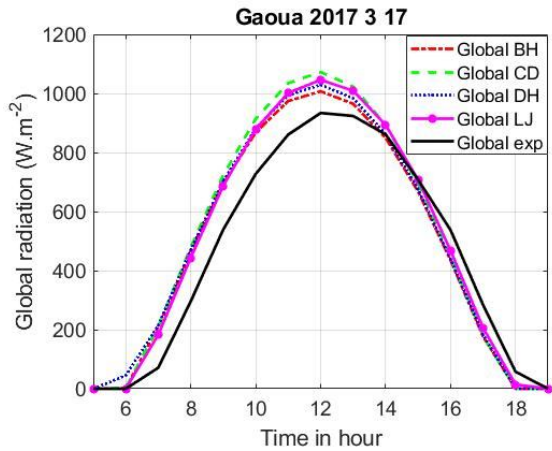


Figure 20: Comparison between the measured radiation and the simulated radiation of the three (03) theoretical models on 3/17/2017 in Gaoua

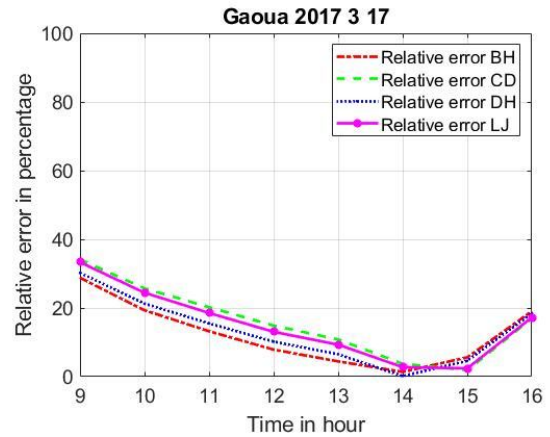


Figure 21: Relative error between the measured radiation and the simulated radiation of the three (03) models on 3/17/2017 in Gaoua

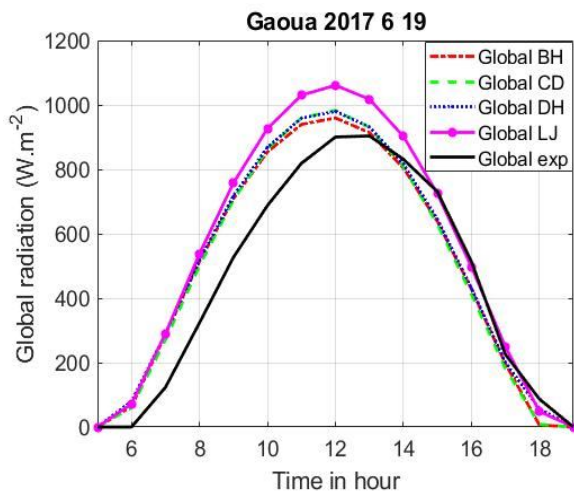


Figure 22: Comparison between the measured radiation and the simulated radiation of the three (03) theoretical models on 1/18/2017 in Gaoua

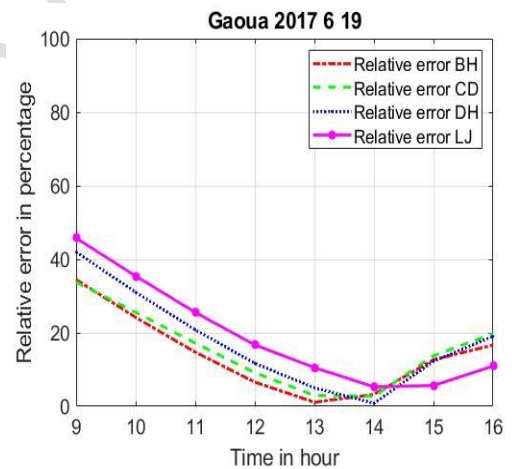


Figure 23: Relative error between the measured radiation and the simulated radiation of the three (03) models on 18/01/2017 in Gaoua

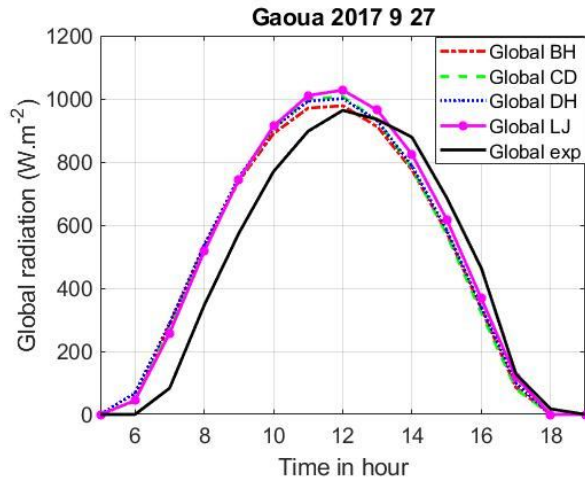


Figure 24: Comparison between the measured radiation and the simulated radiation of the three (03) theoretical models on 15/10/2017 in Gaoua

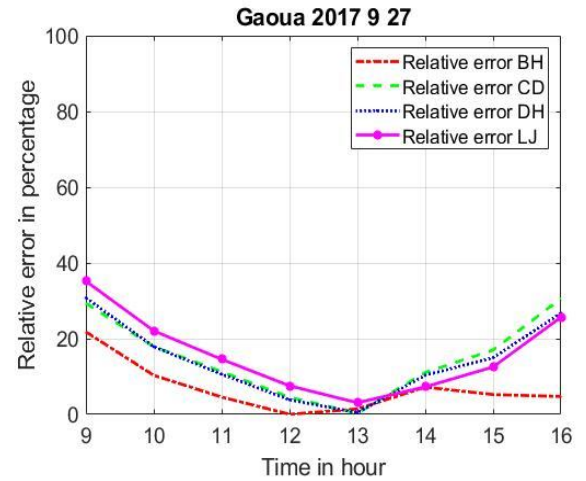


Figure 25: Relative error between the measured radiation and the simulated radiation of the three (03) models for the day of 15/15/2017 in Gaoua

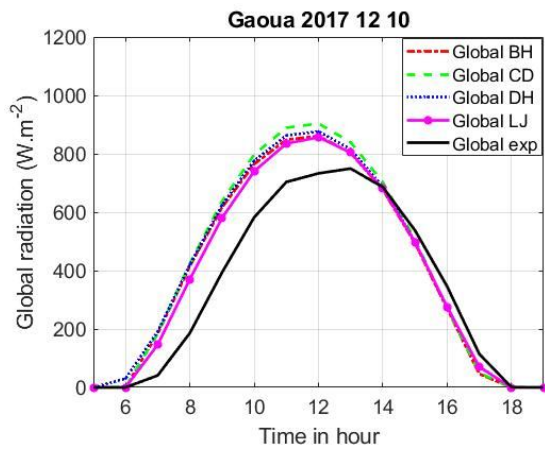


Figure 26: Comparison between the measured radiation and the simulated radiation of the three (03) theoretical models on 10/12/2017 in Gaoua

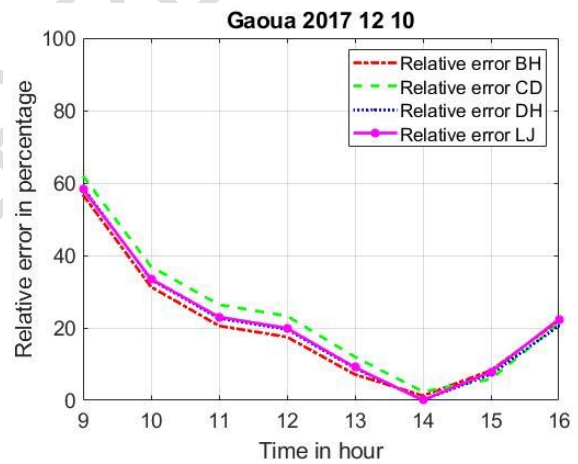


Figure 27: Relative error between the measured radiation and the simulated radiation of the three (03) models on 10/12/2017 in Gaoua

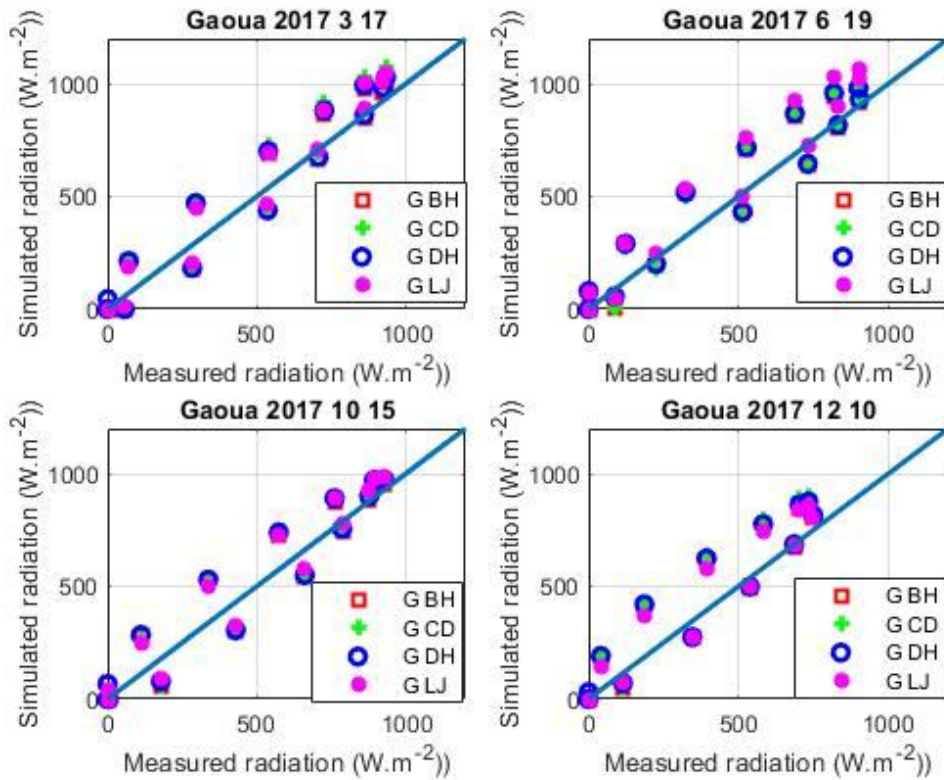


Figure 28: Simulated radiation as a function of measured radiation for the city of Gaoua

3.1.4 Statistical Indicators

Table 3: Statistical indicators of the four models and for the different chosen days of the year for the three cities

Models		Day	17-Apr	29-July	15-Sept	10-Dec
Dori	Bird and Hulstrom	NMAE(%)	7,70	3,80	6,50	1,90
		NRMSE(%)	11,20	5,70	8,00	1,80
	Capderou	NMAE(%)	11,80	4,00	6,90	4,90
		NRMSE(%)	15,50	5,30	9,00	5,50
	Davy and Hay	NMAE(%)	10,30	7,40	9,30	2,60
		NRMSE(%)	11,80	7,10	10,40	5,10
	Lui & Jordan	NMAE(%)	14,40	12,90	13,50	2,50
		NRMSE(%)	18,20	16,80	17,10	2,50
Models		Day	16-Mar	30-June	15-Sept	10-Dec
Ouaga	Bird and Hulstrom	NMAE(%)	34,90	25,10	20,70	18,30
		NRMSE(%)	44,10	33,60	25,80	21,20
	Capderou	NMAE(%)	41,70	22,20	19,90	23,10

		NRMSE(%)	53,50	30,30	26,20	27,10
Gaoua	Davy and Hay	NMAE(%)	25,80	24,50	21,80	19,90
		NRMSE(%)	46,90	31,90	27,80	23,30
	Lui & Jordan	NMAE(%)	39,90	33,00	26,60	19,70
		NRMSE(%)	51,20	43,80	35,00	23,20
	Models	Day	17-Mar	19-June	15-Oct	10-Dec
	Bird and Hulstrom	NMAE(%)	16,90	17,60	18,30	28,00
		NRMSE(%)	19,10	22,10	20,10	33,80
	Capderou	NMAE(%)	20,70	18,50	19,10	31,70
		NRMSE(%)	24,40	22,60	21,30	38,70
	Davy and Hay	NMAE(%)	17,90	21,80	19,00	28,60
		NRMSE(%)	20,60	27,00	20,90	35,50
	Lui & Jordan	NMAE(%)	19,70	22,80	19,70	28,90
NRMSE(%)		23,10	30,10	22,70	35,50	

3.2 DISCUSSION

The curves in Figures 2 to 28 represent on the one hand the radiated simulated and measured as a function of true solar time (TSV), on the other hand the curves of the relative errors between the radiation simulated and measured as a function of time and finally the simulated radiation versus measured radiation. Overall, the shapes of the measured and simulated radiation curves are the same and vary during the day. All the curves have the shape of a bell for the three cities and for the day of the different months of the year. For the cities of Dori and Ouaga, the simulated and measured curves are practically in phase throughout the day, but for those of Gaoua, a slight phase shift is observed between the simulated and measured curves and this results in the observation of points of intersection in the figures. The values of the simulated and measured radiation are low at sunrise and sunset and reach their maximum in the middle of the day. This is in agreement with the course of the sun during a day. The differences between the radiation curves simulated and measured during the day are more pronounced for the city of Ouagadougou than those of Gaoua. For the city of Dori, these differences are relatively smaller than those of the two previous cities. The normalized values of the RMSE and MAE in table 3 confirm this observation. Indeed, the values for the city of Ouagadougou are higher than those of the cities of Gaoua and Dori. The lowest values are observed for the city of Dori and this for all models. Table 3 shows that in all cases, the normalized values of the RMSEs are higher than the normalized values of the MAEs. Jan Kleissl et al [12] raises the issue of the most appropriate magnitude to declare the dispersion error between the RMSE and the MAE. The main difference between the two is that RMSE is determined by the square of the differences, unlike MAE. Therefore, outliers have much more influence on reported accuracy when using the RMSE metric. This is therefore also valid for the normalized values of these quantities.

For the city of Dori, the values of the simulated radiation as a function of the measured radiation show that the points in the graphic representation are very close to the 1st bisector and slightly above it. Similarly, the relative errors during a day are relatively small for the city of Dori. This is not the case of the city of Ouagadougou where the values of the simulated radiations according to the measured radiations are all above the 1st bisector compared to those of the city of Dori. This shows an overestimation of the radiation by the simulated data. The values of relative errors during a day are also higher. The study conducted by Ouédraogo et al [5], and concerning the city of Ouagadougou and over a period of three months in the year 2019, also showed that the model of Liu and Jordan and that of Capderou overestimate the radiation in the

city of Ouagadougou for the chosen study days. For the city of Gaoua, the simulated radiation has higher values in the morning until part of the afternoon and lower for the other part of the afternoon. The observation of the simulated radiation as a function of the measured radiation confirms this. Indeed, part of the points are found above the 1st bisector and the other part below. It is the same for relative errors during a day where the curves decrease until they cancel out in the morning until part of the afternoon, to then increase in the second part of the afternoon. -noon until sunset. For the cities of Dori and Ouagadougou, Guengané et al [7], using data from a typical year in Burkina, showed that the Davies & Hay model underestimates global insolation. But for the Bird & Hulstrom model, the estimated global radiation are very close to the measured values. On the other hand, an underestimation of the peak of sunshine by the Bird & Hulstrom model for the average day of December is noted.

To summarize, the good values of the statistical indicators for the city of Dori can be explained by a good clarity of the sky. Unlike the city of Ouagadougou where the sky is much more polluted. At the level of Ouaga, the overestimates can be attributed to anthropogenic activities. Indeed, in Ouagadougou, pollution linked to human activities is numerous. The large number of motorized vehicles release a lot of gas in nature. In addition, the vast majority of roads are not paved, which generates dust during the movement of motorized vehicles. These dusts and gases released constitute aerosols which contribute to attenuating the solar radiation in the city. The models valid for a clear sky, must be reviewed to take into account the strong contribution of aerosols (which is not the case of the models of Capderou and Liu and Jordan). Gaoua being a city located in the south of the country which is an area experiencing better rainfall than the center and the north, the overestimations of the theoretical models can be explained by the low solar potential and also by the high relative humidity of this area. The increase in relative humidity leads to the suspension of water molecules which further contribute to the reflection of direct radiation. Studies show that aerosols affect the Earth's radiation balance ([19] [20]). Bado and al showed that mixed or intermediate days are the most frequent and are due to a mixture of dust and combustion particles.

A classification of the different models shows that the model of Bird and Hulstrom is the one which comes closest to the measured radiation, followed by that of Davies and Hay and finally by that of Capderou. In the town of Dori, the most appropriate model for estimating solar radiation is therefore that of Bird and Hulstrom. For the cities of Ouagadougou and Gaoua, the different models are not suitable.

4. CONCLUSION

In this article, four (04) models for estimating global solar radiation at hourly intervals on a horizontal plane were studied in three (03) cities of Burkina. These are Dori, Ouagadougou and Gaoua. This work allowed us to compare measured values and those estimated by four parameterized models for the year 2017. Standardized statistical indicators and graphics were used to validate the models. It appears from the study that these models can approach reality with great precision with only a few meteorological data for the city of Dori. But for the cities of Ouagadougou and Gaoua, the calculated statistical indicators show a difference between the simulated values and the measured values. As a result, the models do not properly estimate the radiation in these two cities for the year 2017. Since measurements of direct and diffuse radiation are not available, it was not possible to compare them with those simulated. Such a study would fill the gaps in terms of measurements for the different components of solar radiation in locality where there is not a meteorological agency. It should be remembered that these models studied are specific to days characterized by a state of clear skies. Moreover, the direct use of the models proposed in the literature can lead to an overdimensioning of solar systems. The validation of radiation models is a method of choice before any exploitation.

REFERENCES

- [1] A. H. Pekarek, "Solar Forcing of Earth's Climate", Environ. Geosci., vol. 7, no. 4, p. 215-215, 2000, doi: 10.1046/j.1526-0984.2000.74003-7.x.
- [2] K. Bouchouicha, "Multispectral modeling of satellite images Applications: Quantification of the Soil-Atmosphere energy balance", Department of Engineering Physics, University of Science and Technology of Oran Mohamed-Boudiaf USTOMB, 2017. http://univusto.dz/theses_en_ligne/index.php?lvl=notice_display&id=2271.
- [3] F. Trahi, "Prediction of global solar irradiation for the Tizi ouzou region by artificial neural networks: Application for the dimensioning of a photovoltaic installation for the supply of the LAMPA research laboratory", Thesis, Mouloud Mammeri University, 2011. Accessed: May 26, 2021. [Online]. Available at: <https://dl.ummtto.dz/handle/ummtto/623>
- [4] O. COULIBALY, "Contribution to the development of thermal and energy regulations for buildings in Burkina Faso: Multiparametric basic data and thermo-aeraulic modeling under CoDyBa and TRNSYS", doctoral thesis. University of Ouagadougou, 2011.
- [5] S. Ouédraogo, A. S. Zongo, J.-F. N'Zihou, T. Daho, and A. Béré, "Modeling of incident global solar radiation on a horizontal and inclined plane by four semi-empirical models on the site of the city of Ouagadougou.", J. Phys. SOPHYS, vol. 2, No. 2, 63756374400000000, doi: 10.46411/jpsoaphys.2020.02.25.
- [6] E. Ouédraogo, "Determination of basic climatic data and characterization of compressed earth blocks for the study of thermal comfort in buildings in dry tropical climates", Doctoral thesis, Doctoral School of Science and Technology, University of Ouagadougou, 2015. [En line]. Available at: http://pmb.univ-ouaga.bf/pmb/opac_css/index.php?lvl=notice_display&id=80341
- [7] H. Guengane et al., "Contribution to the estimation of the solar potential on the ground by semi-empirical methods and based on the thermal zoning of Burkina Faso", Asian Journal of Science and Technology Vol. 10, Issue, 12, pp.10545-10555, December, 2019.
- [8] M. Sidibé, D. Soro, W. F. Fassinou, and S. Touré, "Reconstitution of Solar Radiation on a Site of the Littoral in Côte D'ivoire", **INTERNATIONAL JOURNAL OF ENGINEERING RESEARCH AND TECHNOLOGY. ISSN 0974-3154, VOL 10, NUMBER 1 (2017), PP. 19-34**

- [9] D. Saheb-koussa, M. Koussa, and M. Belhamel, "Reconstruction of solar radiation in clear skies", *Revue Energ. Renewables*, vol. 9, no. 2, p. 91-97, June 2006.
- [10] M. Merad née Mesri, A. Cheknane, and R. Ilyes, *Introduction to the Algerian solar field: Theory and applications*. Amar Telidji University – Laghouat- Faculty of Technology Department of Electronics. Accessed: January 14, 2022. [Online]. Available at: https://www.academia.edu/8889767/Introduction_au_gisement_solaire_alg%C3%A9rien
- [11] "Giovanni". <https://giovanni.gsfc.nasa.gov/giovanni/> (accessed January 14, 2022).
- [12] J. Kleissl, T. Hoff, R. Perez, D. Renné, and J. Stein, "Reporting of irradiance modeling relative prediction errors", *Prog. Photovoltaic. Res. Appl.*, vol. 21, p. 1514, Nov. 2013, doi: 10.1002/pip.2225.
- [13] M. Mesri-Merad, I. Rougab, A. Cheknane, and N. I. Bachari, "Estimation of solar radiation on the ground by semi-empirical models", *Renewable Energy Review* Vol. 15 N°3 (2012) 451 - 463.
- [14] M. Iqbal, *An introduction to solar radiation*. 1st ed, Elsevier, 1983.
- [15] R. E. Bird and R. L. Hulstrom, "Simplified clear sky model for direct and diffuse insolation on horizontal surfaces", *Solar Energy Research Inst., United States: N. p.*, 1981. Web. doi:10.2172/6510849.
- [16] G. Robinson, "Absorption of solar radiation by atmospheric aerosol as revealed by Measurements at the Ground", *Arch. For Meteorol. Geophys. Bioklimatol. Ser. B*, Vol. 12, p.19-40, July. 1962, doi: 10.1007/BF02317950.
- [17] A. Brahimi, "Performance study of a flat-water solar collector", other, University of Lorraine, 2016. Consulted on: May 26, 2021. [Online]. Available at: <https://hal.univ-lorraine.fr/hal-01825548>
- [18] F. Yettou, M. Ali, M. Haddadi, and A. Gama, "Comparative study of two models for calculating solar radiation in clear skies in Algeria", *Renewable Energy Review* Vol. 12 N°2 (2009) 331 – 346.
- [19] R. Guebsi, "Impact of water vapor and desert aerosols on the radiation balance and their contributions to the intensification of the thermal depression in West Africa", phdthesis, University Paris Saclay (COMUE), 2017., <https://tel.archives-ouvertes.fr/tel-01582153>
- [20] B. Nébon et al., "Study of Aerosol Impact on the Solar Potential Available in Burkina Faso, West Africa", *International Journal of Environment and Climate Change*, 9(5), 297-310. <https://doi.org/10.9734/ijec/2019/v9i530116>.

DEFINITIONS, ACRONYMS, ABBREVIATIONS

Here is the Definitions section. This is an optional section.

Term: Definition for the term

h	: hour
A	: Constant that depend on the state of the sky
B	: Constant that depend on the state of the sky
BH	: Bird and Hultrom

C	: Constant that depend on the state of the sky
CD	: Capderou
D	: Diffuse
DH	: Davy and Haye
G	: Global
I	: Direct
I_0	: Average solar constant
I_{sc}	: Extraterrestrial solar constant
kWh	: Kilo watt hour
LJ	: Liu and Jordan
m^2	: square meter
m_a	: Corrected optical air mass
MAE	: Mean Absolute Error
m_r	: Relative optical air mass
N	: Number of value
n_j	: Number of day of the year
NMAE	: Normalised Mean Absolute Error
NRMSE	: Normalised Root Mean Square Error
θ_z	: Zenithal distance
RMSE	: Root Mean Square Error
τ_a	: Transmission coefficient after aerosol diffusion
τ_g	: Transmission coefficient after absorption by the permanent gases (CO ₂ et O ₂)
T_L	: Number of ideal atmospheres
τ_o	: Absorption coefficient by the ozone layer
τ_r	: Transmission coefficient after molecular or Rayleigh scattering
TSV	: True solar time
τ_w	: Transmission coefficient after absorption of radiation by water vapour
T_w	: Disturbance due to gaseous absorption
Val _{es}	: estimated value
Val _{me}	: measured value
z	: Altitude of the location

METEOROLOGICAL AGENCY DATA FOR 2017

OUAGA DATA

Hour	Ray_3_16_75	Ray_6_30_181	Ray_9_15_258	Ray_12_10_344
------	-------------	--------------	--------------	---------------

1	0,00	0,00	0,00	0,00
2	0,00	0,00	0,00	0,00
3	0,00	0,00	0,00	0,00
4	0,00	0,00	0,00	0,00
5	0,00	0,00	0,00	0,00
6	0,00	15,30	10,20	5,10
7	101,70	145,00	117,00	61,00
8	330,60	345,90	345,90	244,10
9	544,20	531,50	564,60	460,30
10	684,10	686,70	729,90	628,20
11	740,10	778,20	808,70	709,50
12	773,10	785,80	887,60	745,10
13	712,10	783,30	872,30	714,60
14	610,40	735,00	750,20	630,70
15	457,80	615,40	562,00	457,80
16	272,10	440,00	333,20	249,20
17	134,80	190,70	167,80	83,90
18	25,40	55,90	20,30	0,00
19	0,00	0,00	0,00	0,00
20	0,00	0,00	0,00	0,00
21	0,00	0,00	0,00	0,00
22	0,00	0,00	0,00	0,00
23	0,00	0,00	0,00	0,00
24	0,00	0,00	0,00	0,00

GAOUADATA

Hour	Ray_3_17_76	Ray_6_19_170	Ray_9_27_275	Ray_12_10_344
1	0,00	0,00	0,00	0,00
2	0,00	0,00	0,00	0,00
3	0,00	0,00	0,00	0,00
4	0,00	0,00	0,00	0,00
5	0,00	0,00	0,00	0,00
6	0,00	0,00	0,00	0,00
7	71,00	123,40	82,90	41,00
8	295,80	323,50	345,80	186,20
9	538,90	527,00	574,10	393,30
10	727,20	687,70	769,50	582,20
11	860,50	818,70	897,50	703,40
12	933,70	900,30	963,50	732,90
13	923,70	903,60	934,60	749,40
14	861,20	831,20	878,10	685,90
15	707,70	730,70	686,80	537,90
16	537,20	513,90	463,80	345,80
17	283,90	225,60	128,20	114,30

18	57,50	87,00	17,40	0,70
19	0,00	0,00	0,00	0,00
20	0,00	0,00	0,00	0,00
21	0,00	0,00	0,00	0,00
22	0,00	0,00	0,00	0,00
23	0,00	0,00	0,00	0,00
24	0,00	0,00	0,00	0,00

DORI DATA

Hour	Ray_4_17_107	Ray_6_23_174	Ray_9_15_258	Ray_12_10_344
1	0,00	0,00	0,00	0,00
2	0,00	0,00	0,00	0,00
3	0,00	0,00	0,00	0,00
4	0,00	0,00	0,00	0,00
5	0,00	0,00	0,00	0,00
6	8,00	19,70	5,20	0,00
7	158,80	139,00	161,80	77,70
8	402,70	319,00	406,20	316,80
9	632,80	522,70	639,70	536,50
10	815,80	688,90	814,00	691,60
11	932,80	787,60	927,80	795,10
12	958,40	795,80	965,30	818,90
13	934,20	789,40	902,80	777,60
14	827,90	714,90	794,00	678,40
15	673,00	566,80	620,00	502,80
16	458,10	389,90	396,90	300,80
17	212,70	196,90	167,00	76,40
18	28,20	44,90	10,20	0,00
19	0,00	0,00	0,00	0,00
20	0,00	0,00	0,00	0,00
21	0,00	0,00	0,00	0,00
22	0,00	0,00	0,00	0,00
23	0,00	0,00	0,00	0,00
24	0,00	0,00	0,00	0,00